Neutrino-Driven Jets and Rapid-Process Nucleosynthesis

Shigehiro Nagataki

Department of Physics, School of Science, the University of Tokyo, 7-3-1 Hongo, Bunkyoku, Tokyo 113, Japan

Received _____; accepted _____

ABSTRACT

We have studied whether the jet in a collapse-driven supernova can be a key process for the rapid-process (r-process) nucleosynthesis. We have examined the features of a steady, subsonic, and rigidly rotating jet in which the centrifugal force is balanced by the magnetic force. As for the models in which the magnetic field is weak and angular velocity is small, we found that the r-process does not occur because the final temperature is kept to be too high and the dynamical timescale becomes too long when the neutrino luminosities are set to be high. Even if the luminosities of the neutrinos are set to be low, which results in the low final temperature, we found that the models do not give a required condition to produce the r-process matter. Furthermore, the amount of the mass outflow seems to be too little to explain the solar-system abundance ratio in such low-luminosity models. As for the models in which the magnetic field is strong and angular velocity is large, we found that the entropy per baryon becomes too small and the dynamical timescale becomes too long. This tendency is, of course, a bad one for the production of the r-process nuclei. As a conclusion, we have to say that it is difficult to cause a successful r-process nucleosynthesis in the jet models in this study.

Subject headings: nucleosynthesis, abundances — stars: magnetic — stars: rotation — supernovae: general

1. INTRODUCTION

It is one of the most important astrophysical problems that the sites where the rapid-process (r-process) nucleosyntesis occurs are not still known exactly. There are, at least, three reasons that make the study on r-process nucleosynthesis important. One of them is a very pure scientific interest. The mass numbers of the products of r-process nucleosynthesis are very high (A = 80–250), which means that the most massive nuclei in the universe are synthesized through the r-process. You can guess easily that the situation in which the r-process nuclei are synthesized is a very peculiar one in the universe. We want to know where, when, and how the r-process nuclei are formed. Second reason is that some r-process nuclei can be used as chronometers. For example, the half-lives of ^{232}Th and ^{238}U are 1.405×10^{10} yr and 4.468×10^{9} yr, respectively. So if we can predict the mass-spectrum of the products of r-process nucleosynthesis precisely, we can estimate the ages of metal-poor objects which contain the r-process nuclei by observing its abundance ratio. Third reason is that some r-process nuclei can be used as tools of the study on the chemical evolution in our Galaxy (e.g., Ishimaru and Wanajo 1999), which has a potential to reveal the history of the evolution of our Galaxy itself. Due to the reasons mentioned above, the study on the r-process nucleosynthesis is very important.

The conditions in which the r-process nucleosynthesis occurs successfully are (e.g., Hoffman et al. 1997): (i) neutron-rich ($n_n \geq 10^{20}$ cm^{-3}), (ii) high entropy per baryon, (iii) small dynamical timescale, and (iv) small Y_e. This is because r-process nuclei are synthesized throuth the non-equilibrium process of the rapid neutron capture on the seed nuclei (iron-group elements). In other words, a highly dense, explosive, and neutron–rich site with high entropy will be a candidate for the location where the r-process nucleosynthesis occurs.

The most probable candidates for the sites are collapse-driven supernovae (e.g., Woosley et al. 1994) and/or neutron star mergers (e.g., Freiburghaus et al. 1999). This is because these candidates are thought to have a potential to meet the requirements mentioned above. However, we think that the collapse-driven supernovae are thought to be more probable sites than the neutron star mergers, because metal poor stars already contain the r-process nuclei (e.g., Freiburghaus et al. 1999). In fact, Mcwilliam et al. (1995) reported that the abundance of Eu can be estimated in 11 stars out of 33 metal-poor stars. These observations prove that r-process nuclei are produced from the early stage of the star formation in our Galaxy. Taking the event rate of collapse-driven supernovae (10^{-2} yr^{-1} Gal^{-1}; van den Bergh and Tammann 1991) and neutron star merger (10^{-5} yr^{-1} Gal^{-1}; van den Heuvel and Lorimer 1996; Behte and Brown 1998) into consideration, collapse-driven supernovae are favored since they can supply the r-process nuclei from the early stage of the star formation in our Galaxy. Also, Cowan et al (1999) reported that the abundance ratio of r-process nuclei in metal poor stars are very similar to that in the solar system. This proves that r-process nuclei are synthesized through the similar conditions. This will be translated that, at least, most of the r-process nuclei are from one candidate. So we assume in this paper that most of the r-process nuclei are synthesized in the collapse-driven supernovae.

There are many excellent and precise analytic and/or numerical calculations on the r-process nucleosynthesis in the collapse-driven supernovae. However, it would be able to be said that there is no report that the r-process nuclei can be reproduced completely. For example, Takahashi et al. (1994) performed numerical simulations assuming Newtonian gravity and reported that entropy per baryon in the hot bubble is about 5 times smaller than the required value. Qian and Woosley (1996; hereafter QW96) also reported analytic treatments of the neutrino-driven winds from the surface of the proto-neutron star. At the same time, their analytical treatments are tested and confirmed by numerical methods. However, the derived entropy by their wind solutions are shown to fall short, by a factor

of 2–3, of the value required to produce a strong r-process (Hoffman et al. 1997). Otsuki et al. (2000) have surveyed the effects of general relativity parametrically. They reported that r-process can occur in the strong neutrino-driven winds ($L_\nu \sim 10^{52}$ erg s^{-1}) as long as a massive ($\sim$2.0 $M_\odot$) and compact ($\sim$ 10 km) proto-neutron star is formed. It is very interesting because such a solution can not be found in the frame work of Newtonian gravity (Qian and Woosley 1996). Such a solution is confirmed by the excellent numerical calculations (Sumiyoshi et al. 1999). However, the equation of state (EOS) of the nuclear matter has to be too soft to achieve such conditions. In fact, the r-process nuclei can not be produced in the numerical simulations with an normal EOS (Sumiyoshi et al. 1999).

There is only one report that r-process nucleosynthesis occurred successfully. That is the work done by Woosley et al (1994; here after WWMHM94). In their numerical simulation, the entropy per baryon becomes higher and higher as the time goes on. Finally, at very late phase of neutrino-driven wind ($\sim$ 10 s after the core-collapse), successful r-process occurs. However, there are some questions on their results. One is that the reason why the entropy per baryon becomes high at the late phase is unclear. In fact, when we adopt the analytic formulation of QW96, it is concluded that such a high entropy should not be obtained. It is true that general relativistic effects are included in WWMHM94, but such a high entropy could not be obtained in the work done by Otsuki et al (2000). So the discrepancy between WWMHM94 and QW96 can not be explained by the general relativistic effects alone. Also, WWMHM94 has a problem that the nuclei whose mass numbers are $\sim$ 90 are much produced in the early stage of the neutrino-driven winds. So if we try to reproduce the mass-spectrum of the solar system abundances, we have to abandon the matter which is made at the early stage of the neutrino-driven winds. Even worse, the successful mass-spectrum at the late phase of neutrino-driven winds is destroyed when the reactions of neutral-current neutrino spallations of nucleons from ^{4}He are taken into consideration (Meyer 1995). In their paper, it is reported that (30–50)%

increase in the entropy is needed in order to restore the $A = 195$ peak, which is extremely large modifications to the model. So, although the work done by WWMHM94 is the very remarkable and interesting one, it would not be concluded that the problem of r-process nucleosynthesis has been solved completely.

Due to the reason mentioned above, it will be natural to think that there may be an (some) effect(s) that will help the r-process nucleosynthesis. There are some papers that mention the effects of jet (Symbalisty 1984; Shimizu, Yamada, & Sato 1994; Nagataki 2000) that is generated around the polar region of the highly rotating (the period $T \sim$1ms) and/or magnetized ($\sim 10^{15}$ G) proto-neutron star (LeBlanc & Wilson 1970; Symbalisty 1984; Shimizu, Yamada, & Sato 1994; Yamada & Sato 1994; Fryer & Heger 1999). Since the physical conditions in the jet are different from those in a spherical explosion, the products of the nucleosynthesis are expected to be different. In fact, it is reported that the products of the explosive nucleosynthesis in a jet-like explosion in Si– and O– rich layer are much different from those in a spherical explosion (Nagataki et al. 1997; Nagataki 2000). So it is natural to think that the products of explosive nucleosynthesis in the Fe core (that is, in the hot bubble) will be also changed due to the effects of the jet. This is the reason why we should examine whether the effects of the jet can help the synthesis of r-process nuclei or not.

Since there is no numerical simulation on the r-process nucleosynthesis in the jet during the neutrino-driven wind phase, our final goal is to perform such realistic numerical simulations. However, such a numerical simulation will be a heavy task. We also think that the results of such numerical simulations will not be understood completely without analytical studies. So, before performing such numerical simulations, we examine the physical conditions of the jet using a simple model. In this paper, we study a steady, subsonic, and rigidly rotating flow of the jet that is driven by neutrinos. We study the

effects of the jet on the physical conditions such as the entropy per baryon and the dynamical timescale. Finally, we discuss whether the effects of the jet can help the synthesis of r-process nuclei.

In section 2, we explain the formulation for the jet in the hot bubble. In section 3, we show the results. Summary and discussions are presented in section 4.

2. FORMULATION OF JET

2.1. Basic Equations

In Gaussian units, the Euler's equation acted on by electromagnetic forces can be written as (Shapiro and Teukolsky 1883)

$$v\frac{dv}{dt} = -\frac{1}{\rho}\nabla P - \nabla\Phi - \frac{1}{8\pi\rho}\nabla B^2 + \frac{1}{4\pi\rho}(\vec{B}\cdot\nabla)\vec{B}. \tag{1}$$

Here

$$\frac{d}{dt} = \frac{\partial}{\partial t} + \vec{v}\cdot\nabla \tag{2}$$

is the Lagrangian time derivative following a fluid element.

In this paper, we study a steady jet which has ϕ-symmetry around the polar region of the proto-neutron star. So we use the cylindrical coordinate (r, ϕ, z) for convenience. The origin z=0 is set at the center of the proto-neutron star. In the cylindrical coordinate, the Euler equation can be written as

$$\begin{pmatrix} v_r\frac{\partial v_r}{\partial r} + v_z\frac{\partial v_r}{\partial z} - \frac{v_\phi^2}{r} \\ v_r\frac{\partial v_\phi}{\partial r} + v_z\frac{\partial v_\phi}{\partial z} + \frac{v_r v_\phi}{r} \\ v_r\frac{\partial v_z}{\partial r} + v_z\frac{\partial v_z}{\partial z} \end{pmatrix} = -\frac{1}{\rho}\begin{pmatrix} \frac{\partial P}{\partial r} \\ 0 \\ \frac{\partial P}{\partial z} \end{pmatrix} - \begin{pmatrix} 0 \\ 0 \\ \frac{GM}{z^2} \end{pmatrix} + \frac{1}{4\pi\rho}\begin{pmatrix} \left(\frac{\partial B_r}{\partial z} - \frac{\partial B_z}{\partial r}\right)B_z - \frac{B_\phi}{r}\frac{\partial}{\partial r}(rB_\phi) \\ \frac{B_r}{r}\frac{\partial}{\partial r}(rB_\phi) + B_z\frac{\partial B_\phi}{\partial z} \\ -B_r\left(\frac{\partial B_r}{\partial z} - \frac{\partial B_z}{\partial r}\right) - B_\phi\frac{\partial B_\phi}{\partial z} \end{pmatrix}. \tag{3}$$

Conservation of mass requires that

$$\dot{M} = \int_0^D 2\pi r \rho v_z dr, \tag{4}$$

where $\dot{M}$ and D are the constant mass outflow rate in the ejecta and the radius of the jet, respectively.

The equation for the evolution of material energy, ϵ, is

$$\begin{aligned} \rho\dot{q} &= \nabla\cdot(\rho\epsilon\vec{v}) + P\nabla\cdot\vec{v} & (5)\\ &= \left(\frac{1}{r}\frac{\partial}{\partial r}(r\rho\epsilon v_r) + \frac{\partial}{\partial z}(\rho\epsilon v_z)\right) + P\left(\frac{1}{r}\frac{\partial}{\partial r}(rv_r) + \frac{\partial}{\partial z}v_z\right) & (6)\end{aligned}$$

where $\dot{q}$ is the net specific heating rate due to neutrino interactions (Qian and Woosley 1996). In this study, we consider three neutrino heating and/or cooling processes (neutrino absorption on free nucleons, neutrino scattering processes on the electrons and positrons, and electron capture on free nucleons) as

$$\dot{q} = \dot{q}_{\nu N} + \dot{q}_{\nu e} - \dot{q}_{eN}, \tag{7}$$

where

$$\dot{q}_{\nu N} = 1.55\times10^{-5} N_{\rm A}\left[(1-Y_e)L_{\nu_e,51}\epsilon^2_{\nu_e,{\rm MeV}} + Y_e L_{\bar{\nu}_e,51}\epsilon^2_{\bar{\nu}_e,{\rm MeV}}\right]\frac{1-x}{R_6^2} \quad \left[{\rm erg\ s^{-1}\ g^{-1}}\right], \tag{8}$$

$$\dot{q}_{\nu e} = 3.48\times10^{-6} N_{\rm A}\frac{T^4_{\rm MeV}}{\rho_8}\left(L_{\nu_e,51}\epsilon_{\nu_e,{\rm MeV}} + L_{\bar{\nu}_e,51}\epsilon_{\bar{\nu}_e,{\rm MeV}} + \frac{6}{7}L_{\nu_\nu,51}\epsilon_{\nu_\nu,{\rm MeV}}\right)\frac{1-x}{R_6^2} \quad \left[{\rm erg\ s^{-1}\ g^{-1}}\right], \tag{9}$$

and

$$\dot{q}_{eN} = 3.63\times10^{-6} N_{\rm A} T^6_{\rm MeV} \quad \left[{\rm erg\ s^{-1}\ g^{-1}}\right]. \tag{10}$$

Here R_6 is the neutrino sphere radius in units of 10^6 cm, $x = (1-R^2/z^2)^{1/2}$, $N_{\rm A}$ is Avogadro's number, $L_{\nu,51}$ is the individual neutrino luminosity in 10^{51} erg s^{-1}, $\epsilon_{\nu,{\rm MeV}}$ is an appropriate neutrino energy ϵ_ν in MeV (Qian and Woosley 1996). In this study, we set $\dot{q}$=0

at $T \leq$0.5 MeV, because free nucleons are bound into α-particles and heavier nuclei and electron-positron pairs annihilate into photons.

The pressure P and internal energy ϵ are determined approximately by the relativistic electrons and positrons and photon radiation as long as $T \geq 0.5$ MeV. So the pressure and internal energy can be written as

$$P = \frac{11\pi^2}{180}\frac{k^4T^4}{\hbar^3c^3} \quad \left[\mathrm{dyn\ cm^{-2}}\right] \tag{11}$$

and

$$\epsilon = \frac{11\pi^2}{60}\frac{k^4T^4}{\hbar^3c^3\rho} \quad \left[\mathrm{erg\ g^{-1}}\right], \tag{12}$$

where k and $\hbar$ are Boltzmann and Planck constants, respectively. These are the basic equations in this paper. Precisely, we should consider the effects of annihilations of electron-positron pairs on the dynamics at $T \leq 0.5$ MeV. However, its effects seems to be little (Sumiyoshi et al. 1999).

2.2. Model for the Jet

In this study, we try to construct a simple steady state for a jet so that we can understand the effects of magnetic fields clearly. So we assume in this study that the form of the magnetic fields is

$$\vec{B} = (0, 0, B_\phi(r, z)). \tag{13}$$

Next, we seek a solution for the jet rotating rigidly. That is, we seek a solution $\vec{v} =$ $(0,\Omega r,v_z(r, z))$ at $z \geq R$, where Ω is the angular velocity of the proto-neutron star. From Eq. (3), $\vec{B}$ and $\vec{v}$ must meet the following relation:

$$\begin{pmatrix} -\Omega^2 r \\ v_z\frac{\partial v_z}{\partial z} \end{pmatrix} = -\frac{1}{\rho}\begin{pmatrix} \frac{\partial P}{\partial r} \\ \frac{\partial P}{\partial z} \end{pmatrix} - \begin{pmatrix} 0 \\ \frac{GM}{z^2} \end{pmatrix} - \frac{1}{4\pi\rho}\begin{pmatrix} \frac{B_\phi}{r}\frac{\partial}{\partial r}(rB_\phi) \\ B_\phi\frac{\partial B_\phi}{\partial z} \end{pmatrix}. \tag{14}$$

In this case, there is a useful approximate solution. That is,

$$B_\phi = (2\pi\rho)^{\frac{1}{2}}\Omega r, \tag{15}$$

where ρ and P are assumed to be a function of z alone. It is noted that this approximate solution is valid as long as ΩD is small enough. In fact, the derivatives of ρ and T by z can be written as

$$\frac{d\rho}{dz} = -\frac{\frac{P\dot{q}}{v_z\epsilon} + \frac{\rho GM}{z^2}}{\frac{P}{\epsilon\rho}\left(\epsilon + \frac{P}{\rho}\right) - v_z^2 + \frac{(\Omega r)^2}{4}} \tag{16}$$

$$\frac{dT}{dz} = \frac{\frac{\dot{q}}{v_z} + \left(\frac{\epsilon}{\rho} + \frac{P}{\rho^2}\right)\frac{d\rho}{dz}}{\frac{4\epsilon}{T}}. \tag{17}$$

It is clearly understood from Eq. (16) that the solution holds valid as long as ΩD is small enough. In this case, Eq. (4) can be rewritten as

$$\dot{M} = \pi D^2 \rho v_z. \tag{18}$$

From Eqs. (14) and (15), we can see that the magnetic fields accelerate the matter as long as the density gradient is negative. We are also able to see clearly from Eq. (15) that small ΩD corresponds to weak magnetic field. So we call such solutions weak field solutions in this paper. On the other hand, we also want to see what can happen as the magnetic fields are getting stronger and stronger. So, although the truth is that these solutions are inapplicable to the case of strong magnetic fields, we extend these solutions to the case in which ΩD is relatively large. By so doing, we will be able to find at least what happens in the case of strong magnetic fields qualitatively. We call such solutions strong field solutions in this paper. In section 3, we show the results for the weak and strong field solutions, respectively.

2.3. Boundary Conditions

In this study, the surface of the proto-neutron star is considered as the inner boundary. The inner boundary conditions are composed of density, luminosities of neutrinos, mass and radius of the proto-neutron star, velocity of the outflow, and ΩD. Initial temperature and final electron fraction are determined by these parameters as (Qian and Woosley 1996)

$$T_i = 1.19 \times 10^{10} \left[1 + \frac{L_{\nu_e}}{L_{\bar{\nu}_e}} \left(\frac{\epsilon_{\nu_e,\mathrm{MeV}}}{\epsilon_{\bar{\nu}_e,\mathrm{MeV}}} \right)^2 \right]^{\frac{1}{6}} L_{\bar{\nu}_e,51}^{\frac{1}{6}} R_6^{-\frac{1}{3}} \epsilon_{\bar{\nu}_e,\mathrm{MeV}}^{\frac{1}{3}} \quad [\mathrm{K}] \tag{19}$$

and

$$Y_{e,f} = \left(1 + \frac{L_{\bar{\nu}_e}}{L_{\nu_e}} \frac{\epsilon_{\bar{\nu}_e,\mathrm{MeV}} - 2\Delta + 1.2\Delta^2/\epsilon_{\bar{\nu}_e,\mathrm{MeV}}}{\epsilon_{\nu_e,\mathrm{MeV}} + 2\Delta + 1.2\Delta^2/\epsilon_{\nu_e,\mathrm{MeV}}} \right)^{-1}, \tag{20}$$

where $L_{\nu,51}$ is the individual neutrino luminosity in 10^{51} ergs s^{-1}, R_6 is the neutron star radius in 10^6 cm, $\Delta = 1.293$ MeV is the neutron-proton mass difference, and $\epsilon_{\nu,\mathrm{MeV}}$ is a neutrino energy in MeV. We assume that the neutron star radius is equal to the neutrino sphere radius.

In this study, the luminosities of neutrinos are assumed to be common (Qian and Woosley 1996; Otsuki et al. 2000). The energy of neutrinos are assumed to be 12, 22, and 34 MeV for ν_e, $\bar{\nu}_e$, and other neutrinos, respectively (Woosley et al. 1994; Qian and Woosley 1996; Otsuki et al. 2000). Surface density is assumed to be 10^{10} g cm^{-3} (Otsuki et al. 2000). Initial velocity of the outflow is chosen so that $\dot{M}$ becomes less than $\dot{M}_{\mathrm{crit}}$, where $\dot{M}_{\mathrm{crit}}$ is the critical value for supersonic solution. We have to emphasize that the flow is assumed to be subsonic and contain no critical point. Previous works also adopted this assumption (Qian and Woosley 1996; Otsuki et al. 2000). In case we try to survey the flow that contains a transition point like a shock front, we can not use Eqs. (6), (14), (16), and (17). This is because these differential equations diverge and break down. In order

to treat such a flow that contains a discontinuity, we have to use the Rankine-Hugoniot relation instead of these equations. We will examine such flows in the forthcoming paper. D is assumed to be 10^5 cm, which is about one tenth of the proto-neutron star radius. We note that an appropriate environment can exist around the jet, that is, there is a solution that meets Eq. (14) for $r \geq D$ in which B_ϕ and v_ϕ becomes zero at $r \to \infty$. So the rigid rotating flow at $r \leq D$ is not an unrealistic solution at all. In this study, we consider only the region $r \leq D$ in which the matter rotates rigidly for simplicity. Other parameters are changed parametrically. The parameters employed as well as the model names are given in Table 1. We take $z = 10^9$ cm for the radius of the outer boundary (Otsuki et al. 2000). Since the radius of the Fe core is about 10^8 cm, we think the radius of the outer boundary is large enough to investigate the r-process nucleosynthesis that occurs in the hot bubble.

EDITOR: PLACE TABLE 1 HERE.

3. RESULTS

3.1. Weak Field Solutions

Output parameters are shown in Table 2. Entropy per baryon (S), dynamical timescale ($\tau_{\rm dyn}$), analytically estimated dynamical timescale ($\tau_{\rm dyn.ana}$), electron fraction (Y_e), and temperature (T) at the outer boundary ($z = 10^9$ cm) are shown in the table. Entropy per

baryon in radiation dominated gas can be written as

$$S/k = \frac{11\pi^2}{45}\frac{k^3}{\hbar^3 c^3}\frac{T^3}{\rho/m_N} \tag{21}$$

as long as $T \geq 0.5$ MeV. m_N is the nucleon rest mass. Even if the annihilation of the electron-positron pairs occurs, the entropy per baryon is conserved. The definition of the dynamical timescale is the time for the temperature to decrease from 0.5 MeV to 0.2 MeV. This is because r-process nucleosynthesis occurs in this temperature range (Woosley et al. 1994; Takahashi et al. 1994; Qian and Woosley 1996). The reason why the dynamical timescales are not written in some models is that temperature does not decrease to 0.2 MeV within $z = 10^9$ cm. The definition of the analytically estimated dynamical timescale is described later (see Eq. (31)).

EDITOR: PLACE TABLE 2 HERE.

There is a tendency that S and T_b in the models studied here are higher than those in the models of QW96. For example, we show in Figure 1 the outflow velocity, temperature, and density as a function of z for Model 10CW and Model 10C in QW96. The inner boundary conditions in Model 10C in QW96 is same as those in Model 10CW (see table 1 in Qian and Woosley 1996). From this figure and Eq. (21), we can see the tendency mentioned above clearly. We consider the reason for this tendency below. In order to find a clue to it, we show the absolute values (in cgs units) of the components in Eqs. (16) and (17) for Model 10CW in Figure 2. From this figure, we can see what determines the gradients of temperature and density. For comparison, we also show those for Model 10C in QW96 in Figure 3. Lines (a)-(g) correspond to $4\epsilon/T$, $(P/\epsilon\rho)(\epsilon + P/\rho)$, v_z^2, $\rho GM/z^2$, $P\dot{q}/v_z\epsilon$, $(\epsilon/\rho + P/\rho^2)\frac{d\rho}{dz}$, and $\dot{q}/v_z$ as a function of z, respectively. As can be seen from Figures 2 and 3, $d\rho/dz$ can be approximated by

$$\frac{d\rho}{dz} \sim -\frac{\frac{\rho GM}{z^2}}{\frac{P}{\epsilon\rho}\left(\epsilon + \frac{P}{\rho}\right)}. \tag{22}$$

Also, dT/dz can be approximated by

$$\frac{dT}{dz} \sim \frac{\left(\frac{\epsilon}{\rho} + \frac{P}{\rho^2}\right)\frac{d\rho}{dz}}{\frac{4\epsilon}{T}} \sim -\frac{m_N}{S}\frac{GM}{z^2}. \tag{23}$$

From Eq. (23) we can see that the temperature gradient dT/dz is steeper when the entropy per baryon is smaller. So we can expect that the entropy per baryon is larger in Model 10CW than Model 10C in QW96. It is verified in Figure 4. So, the problem why T_b becomes high is translated to the problem why the entropy per baryon becomes high in Model 10CW. The answer is shown in Figure 2. The velocity at small radii in Model 10CW is smaller than that in Model 10C in QW96. The entropy per baryon is getting larger with time as long as the heating process is effective. The heating process is effective only at small radii, which is proved in Figure 4. So, if the velocity at small radii is small, there is a long time for the outflow matter to get heat from neutrinos. As a result, higher entropy per baryon can be achieved and T_b becomes higher. This is the case with the jet models studied in this paper. As for the reason why the initial velocity has to be smaller in Model 10CW than Model 10C in QW96 is relatively difficult. At least, we can say that dv_z/dz can be written from Eq. (18) as

$$\frac{dv_z}{dz} = -\frac{v_z}{\rho}\frac{d\rho}{dz} \quad \text{in Model 10CW.} \tag{24}$$

On the other hand, it can be written as

$$\frac{dv_z}{dz} = -\frac{v_z}{\rho}\frac{d\rho}{dz} - \frac{v_z}{r} \quad \text{in Model 10C in QW96,} \tag{25}$$

because $4\pi z^2 \rho v_z$ is constant in Model 10C in QW96. Taking these equations and Eq. (16), which also holds in the models in QW96 (Qian and Woosley 1996), into consideration, the velocity gradient is steeper in Model 10CW as long as $v_z(z)$, $\rho(z)$, and $T(z)$ are same in both models. So we can guess that initial v_z has to be smaller in Model 10CW so as not to achieve the adiabatic sound speed, $v_s = (4P/3\rho)^{\frac{1}{2}}$. This will be the reason why the initial velocity in Model 10CW has to be smaller.

EDITOR: PLACE FIGURE 1 HERE.

EDITOR: PLACE FIGURE 2 HERE.

EDITOR: PLACE FIGURE 3 HERE.

EDITOR: PLACE FIGURE 4 HERE.

Next, we consider the dynamical timescale. As mentioned above, the dynamical timescale becomes infinity when T_b is above 0.2 MeV. Since T_b in the jet models tends to be higher, we can not determine the dynamical timescale in many jet models. This is a bad tendency to produce r-process nuclei. From Table 2, the dynamical timescale can be determined as long as $L_{\bar{\nu}_e,51}$ is small. We will discuss later whether r-process can occur or not in such models. Before we continue to further discussion, we explain the way to derive the analytically estimated dynamical timescale $\tau_{\rm dyn,ana}$.

Like Model 10C in QW96, from Eqs. (6) and (14) we can derive the following equation as long as ΩD is small:

$$\dot{q} = v_z \frac{d}{dz}\left(\frac{v_z^2}{2} + \frac{TS}{m_N} - \frac{GM}{z}\right). \tag{26}$$

So, when the heating/cooling process becomes non-effective, there is a conserved quantum

$$\epsilon_{\rm flow,f} = \left(\frac{v_z^2}{2} + \frac{TS}{m_N} - \frac{GM}{z}\right). \tag{27}$$

In the subcritical case, $v_z \leq v_s$ everywhere, we can approximate Eq. (27) as

$$\frac{TS}{m_N} - \frac{GM}{r} \sim \frac{T_b S}{m_N}. \tag{28}$$

When $T_b \ll 0.5$MeV, we can take

$$\frac{TS}{m_N} \sim \frac{GM}{r} \text{ at } 0.5\text{MeV}. \tag{29}$$

See Qian and Woosley (1996) for details. In this case, $T \propto r^{-1}$ near $T \sim 0.5$ MeV because S is also a conserved quantum as long as the heating/cooling process does not work. From Eq. (21), $\rho \propto r^{-3}$. From Eq. (18), $v_z \propto r^3$. So, $\tau_{\rm dyn,ana}$ can be approximated as

$$\tau_{\rm dyn,ana} = \int_{T=0.5\rm MeV}^{T=0.2\rm MeV} dt = \int_{T=0.5\rm MeV}^{T=0.2\rm MeV} \frac{dt}{dz}\frac{dz}{dT} dT \tag{30}$$

$$= \left(\frac{r}{vT^2}\right)_{T=0.5\rm MeV} \int_{T=0.2\rm MeV}^{T=0.5\rm MeV} T dT \sim 0.42 \left(\frac{r}{v}\right)_{T=0.5\rm MeV} \quad [s]\,. \tag{31}$$

For further discussion, we try to express the dynamical timescale by input parameters (see Qian and Woosley 1996 for details). From simple calculations, we can derive the entropy per baryon and the mass outflow rate in Model 10CW as

$$S/k \sim 235 L_{\bar{\nu}_e,51}^{-\frac{1}{6}} \epsilon_{\bar{\nu}_e,\rm MeV}^{-\frac{1}{3}} R_6^{-\frac{2}{3}} \left(\frac{M}{1.4M_\odot}\right) \tag{32}$$

and

$$\dot{M} \sim \frac{D^2}{4R^2} \times 1.14 \times 10^{-10} L_{\bar{\nu}_e,51}^{\frac{5}{3}} \epsilon_{\bar{\nu}_e,\rm MeV}^{\frac{10}{3}} R_6^{\frac{5}{3}} \left(\frac{1.4M_\odot}{M}\right)^2 \quad \left[M_\odot\ s^{-1}\right], \tag{33}$$

respectively. At last, we can derive the expression for $\tau_{\rm dyn,ana}$ from Eqs. (18), (21), (29), (31), (32), and (33) that

$$\tau_{\rm dyn,ana} \sim 10.5 L_{\bar{\nu}_e,51}^{-\frac{4}{3}} \epsilon_{\bar{\nu}_e,\rm MeV}^{-\frac{8}{3}} R_6^{\frac{5}{3}} \left(\frac{M}{1.4M_\odot}\right) \quad [s]\,. \tag{34}$$

This value for each model is written in Table 2. We can find that $\tau_{\rm dyn,ana}$ agrees with $\tau_{\rm dyn}$ within a factor of 2-3 in all models in which the dynamical timescale can be defined, although $\tau_{\rm dyn,ana}$ tends to be smaller. This precision of $\tau_{\rm dyn,ana}$ is about the same that in the analysis in QW96 (see Qian and Woosley 1996 for details).

We compare $\tau_{\rm dyn,ana}$ derived here with that in QW96 in order to see the effects of jet. It is written as

$$\frac{\tau_{\rm dyn,ana}}{\tau_{\rm dyn,QW}} = 0.15 \frac{R_6^{\frac{2}{3}}}{L_{\bar{\nu}_e,51}^{\frac{1}{3}} \epsilon_{\bar{\nu}_e,\rm MeV}^{\frac{2}{3}}}. \tag{35}$$

For example, when $L_{\bar{\nu}_e,51} = 0.1$, $R_6 = 1$, and $\epsilon_{\bar{\nu}_e,\rm MeV} = 22$, $\tau_{\rm dyn}/\tau_{\rm dyn,QW} = 0.04$. Even if we take the uncertainty (a factor of 2-3) of $\tau_{\rm dyn,ana}$ into consideration, it seems that short dynamical timescale can be realized in jet models. So, as long as T_b can be small (that is, $L_{\bar{\nu}_e,51}$ is small enough), we think that short dynamical timescale can be realized in jet models.

Now we discuss whether r-process nucleosynthesis can occur in jet models or not. We can use the Hoffman's criterion (Hoffman et al. 1997) for the judgment. The Hoffman's criterion can be written as

$$S \geq 2 \times 10^3 Y_e \left(\frac{\tau_{\rm dyn}}{s} \right)^{\frac{1}{3}} \tag{36}$$

for $Y_e \geq$0.38. This is the criterion for production of r-process nuclei with mass number $A \sim$200 (Hoffman et al. 1997). Substituting Eqs. (32) and (34) into Eq. (36), We can translate the criterion into

$$R_6 \leq \frac{0.74}{C^{\frac{3}{11}}} L_{\bar{\nu}_e,51}^{\frac{5}{22}} \left(\frac{M}{1.4 M_\odot} \right)^{\frac{6}{11}}, \tag{37}$$

where $\epsilon_{\bar{\nu}_e,\rm MeV}$ is assumed to be 22. C is the factor 2-3 which represents the tendency that $\tau_{\rm dyn,ana}$ tends to be smaller than $\tau_{\rm dyn}$. In case of M=1.4$M_\odot$ and C=2, we can see from Eq. (37) that R_6 can be larger than 1 as long as $L_{\bar{\nu}_e,51}$ is larger than 8.6. This means that there seems to be possible to produce r-process nuclei without unrealistically soft EOS as long as $L_{\bar{\nu}_e,51}$ is larger than 8.6. However, we found from Table 2 that T_b can not be lower than 0.2 MeV when the neutrino luminosity is so high. So we have to conclude that r-process can not occur in these models.

However, we can find that the requirement to produce r-process nuclei is relaxed in these jet models. In fact, for the models of QW96, the criterion like Eq. (37) can be written as

$$R_{6,\mathrm{QW}} \leq 0.19 L_{\bar{\nu}_e,51}^{\frac{1}{6}} \left(\frac{M}{1.4M_\odot}\right)^{\frac{2}{3}}. \tag{38}$$

So, $R_{6,\mathrm{QW}}$ can be larger than 1 when $L_{\bar{\nu}_e,51}$ is larger than 2.3×10^4, which can not be realized in numerical simulations of supernovae (Woosley et al. 1994). We can compare the required radius in jet models ($C = 2$) with that in models of QW96 as

$$\frac{R_6}{R_{6,\mathrm{QW}}} = 3.2 L_{\bar{\nu}_e,51}^{\frac{2}{33}} \left(\frac{M}{1.4M_\odot}\right)^{-\frac{4}{33}}. \tag{39}$$

For example, in case of $M = 1.4M_\odot$ and $L_{\bar{\nu}_e,51} = 0.1$, $R_6/R_{6,\mathrm{QW}} = 2.8$. This suggests that the EOS of the nuclear matter has not necessary to be too soft as Otsuki et al (2000) requires, when the jet models are adopted. So, we can conclude that the requirement to achieve r-process nucleosynthesis is relaxed for the jet models, although r-process nucleosynthesis is not still able to occur in the jet models. When we include the effects of a jet and general relativity at the same time, an successful solution may be obtained. We will discuss this topic in the forthcoming paper.

Finally, we consider the mass outflow rate. Taking the event rate of collapse-driven supernovae (10^{-2} yr^{-1} Gal^{-1}; van den Bergh and Tammann 1991), one needs 10^{-6} to 10^{-4} $M_\odot$ of ejected r-process material per collapse-driven supernova event to explain the observed solar-abundance ratio (Käppeler et al. 1989; Woosley et al. 1994). We give a rough estimate whether each model can produce r-process matter enough to explain the solar-system abundance. Taking the gravitational binding energy of a neutron star is $\sim 3 \times 10^{53}$ erg into consideration, the duration time, t, can be roughly estimated as

$$t \leq \frac{300}{6 \times L_{\bar{\nu}_e,51}} \quad [\mathrm{s}] \tag{40}$$

where the factor 6 represents the number of flavor of neutrinos. So required $\dot{M}_{\rm req}$ to explain the solar abundance ratio is

$$\dot{M}_{\rm req} \geq \left(10^{-4} - 10^{-6}\right) M_\odot \times \frac{L_{\bar{\nu}_e,51}}{50} \quad \left[M_\odot\ s^{-1}\right]. \tag{41}$$

So $\dot{M}$ in Table 1 has to meet the relation

$$2 \times \dot{M} \sim \dot{M}_{\rm req} \tag{42}$$

where the factor 2 represents that the matter is ejected from both (north and south) sides of the polar region. We can find from Eq. (41), (42), and Table 1 that low-luminosity models like 10GW-10LW and 30FW-30HW can not meet the relation mentioned above, although the high-luminosity models like 10AW-10FW and 30AW-30EW may be able to meet the relation.

At last we can derive the conclusion. In the framework of the steady neutrino-driven jet with weak magnetic fields, high-luminosity models can not work because T_b becomes high and dynamical timescale becomes too long. Also, low-luminosity models do not present a required condition to produce the r-process nuclei in the framework of Newtonian gravity. Although a successful solution may be obtained when we include the effects of jet and general relativity at the same time, the amount of mass outflow seems to be too little to explain the solar-system abundance ratio in such low-luminosity models. As a conclusion, we have to say that it is difficult to cause a successful r-process nucleosynthesis in the weak field solutions.

3.2. Strong Field Solutions

In this subsection, we examine the models in which $\Omega D \neq 0$. As stated in subsection 2.2, the truth is that the solutions studied in this paper are inapplicable to the case of strong

magnetic fields. However, we want to see what can happen as the magnetic fields are getting stronger and stronger. At the same time, we should investigate the range of application of weak field solutions.

In this study, we consider three models (Model 10GS1-3) for strong field solutions. These are listed in Table 1. The strength of the magnetic fields corresponds to 2.5×10^{13} G, 2.5×10^{14} G, and 2.5×10^{15} G, respectively (see Eq. (15)).

The results are shown in Table 2. We can find that the values of output parameters change drastically in Model 10GS3. This result suggests that the weak field solutions can be applied at least in the range of order $B \leq 10^{14}$ G. This means that the weak field solutions will be valid for the typical proto-neutron stars. In case we consider the nucleosynthesis in a magnetar (Woods et al. 1999), we will have to investigate using strong field solutions.

In order to understand what happens in Model 10GS3, we show the outflow velocity, temperature, density, and entropy per baryon as a function of z of Model 10GS3 in Figure 5. We also show the absolute values (in cgs units) of the components of Eqs. (16) and (17) for Model 10GS3 in Figure 6. Lines (a)-(h) correspond to $4\epsilon/T$, $(P/\epsilon\rho)(\epsilon + P/\rho)$, v_z^2, $\rho GM/z^2$, $P\dot{q}/v_z\epsilon$, $(\epsilon/\rho + P/\rho^2)\frac{d\rho}{dz}$, $\dot{q}/v_z$, and $\Omega^2 D^2/4$ as a function of z, respectively. As can be seen from Figures 6, $d\rho/dz$ at $r = D$ can be approximated by

$$\left.\frac{d\rho}{dz}\right|_{r=D} \sim -\frac{\rho GM/z^2}{\Omega^2 D^2/4}. \tag{43}$$

Also, dT/dz can be approximated by

$$\frac{dT}{dz} \sim \frac{T\left(\frac{\epsilon}{\rho} + \frac{P}{\rho^2}\right)\frac{d\rho}{dz}}{4\epsilon} \qquad \text{for } z \leq 8\times10^1 \text{ and } z \geq 2\times10^3 \tag{44}$$

$$\sim \frac{T\dot{q}}{4\epsilon v_z} \qquad \text{for } 8\times10^1 \leq z \leq 2\times10^3. \tag{45}$$

EDITOR: PLACE FIGURE 5 HERE.

EDITOR: PLACE FIGURE 6 HERE.

We note that the denominator of Eq. (43) is $\Omega^2 D^2/4$, which is constant through out. Since the denominator is large, the value of the density gradient becomes small. So the density gradient in 10GS3 becomes nearly zero at smaller z (compare Figures 1 and 5). As a result, temperature does not decrease due to the adiabatic expansion. When the temperature is kept to be high, cooling process works better (see Eqs. (8), (9), and (10)). So, at $z \sim 8 \times 10^6$ cm, the cooling process overcomes the heating process. As a result, entropy per baryon is getting lower in the range $8 \times 10^6 \leq z \leq 2 \times 10^8$ cm. This is the reason why the entropy per baryon becomes small in Model 10GS3. We also note that the temperature gradient becomes too small at $z \geq 2 \times 10^8$ cm. This is because the numerator of Eq. (44) becomes in proportion to $d\rho/dz$, which is very small as seen above. So we can find that the entropy per baryon is small and the dynamical timescale is long in the strong field solution 10GS3. This tendency is a bad one for the production of r-process nuclei. The truth is, of course, that the solutions studied in this paper are inapplicable to the case of strong magnetic fields (see Eq. (16)). However, similar tendency discussed here may be also found in the exact solutions. If so, the strong field solutions are unsuitable for the r-process nucleosynthesis.

Finally we add a comment on the effects of the magnetic fields. You may have thought that the dynamical timescale in the strong field solutions will become shorter than that in the weak field solutions, because the magnetic fields accelerate the matter as long as the density gradient is negative (see Eqs. (14) and (15)). However, in the framework of the steady flow, the density gradient becomes nearly zero and acceleration does not occur. So, the situation may be different and acceleration occurs in the case of an unsteady flow. We will investigate the features of such an unsteady flow by numerical tests in the near future.

4. SUMMARY AND DISCUSSION

We have studied whether the jet in a collapse-driven supernova can be a key process for the r-process nucleosynthesis. We have studied the effects of a jet using a simple model, because the results of a realistic numerical simulation concerning with such a theme will not be understood completely without analytical study. Although our final goal is to perform such realistic numerical simulations, this work is a necessary process to understand the effects of a jet on the r-process nucleosynthesis.

We have studied two cases, that is, the cases in which the magnetic fields are weak/strong. In both cases, we assumed that the flow is steady and subsonic.

As for the weak field solutions, we have concluded that high-luminosity models can not work because T_b becomes high and dynamical timescale becomes too long. Also, low-luminosity models do not present a required condition to produce the r-process nuclei in the framework of Newtonian gravity. Although a successful solution may be obtained when we include the effects of jet and general relativity at the same time, the total mass of the outflow seems to be too little to explain the solar-system abundance ratio in such low-luminosity models. On the other hand, we found that the entropy per baryon is small and the dynamical timescale is long in the strong field solution. We can tell that this tendency is a bad one for the production of r-process nuclei. The truth is that the solutions studied in this paper are inapplicable to the case of strong magnetic fields. However, similar tendency may be also found in the exact solutions. If so, we will be able to conclude that strong field solutions are unsuitable for r-process nucleosynthesis. As a conclusion, we have to say that it seems to be difficult to cause a successful r-process nucleosynthesis in the jet models in this study.

We have to emphasize that there are some assumptions in this study. So, we can not say that we have proved that a successful r-process nucleosynthesis does not occur in a neutrino-driven jet in a collapse-driven supernova. For example, we assumed that the flow is subsonic and there is no critical point, which is the common assumption in the previous studies on the r-process nucleosynthesis (Qian and Woosley 1996; Otsuki et al. 2000). However, we think that we do not need to restrict the solutions in such a way, that is, there may be a transition point at which Eqs. (6), (14), (16), and (17) break down. In most cases, the transition point will be a shock front. It means that the flow will gain entropy at the transition point, which will be a good sense to produce the r-process nuclei. The problem whether the flow contains transition points or not depends sensitively on the initial velocity on the surface of the proto-neutron star. So our final goal is to determine physically the velocity at the surface of the proto-neutron star. It means that the $\dot{M}$ should be not given as an input parameter. It should be an output parameter. We have to investigate the mechanism for determining the outflow velocity at the surface of the proto-neutron star for further discussions. We also assumed that the flow is steady. As seen in subsection 3.2, the density gradient becomes nearly zero and acceleration due to the strong magnetic fields does not occur in the framework of the steady flow. So, the situation may be different and acceleration occurs in the case of the unsteady flow. We should investigate the features of the unsteady jet flow. It will be investigated by numerical tests assuming a simple environment. We will perform such numerical tests in the near future. At the same time, we will try to perform realistic numerical simulations for the jet induced explosion in a collapse-driven supernova and seek a final answer whether the jet in a collapse-driven supernova is a key process for the r-process nucleosynthesis or not.

This research has been supported in part by a Grant-in-Aid for the Center-of-Excellence (COE) Research (07CE2002) and for the Scientific Research Fund (199908802) of the

Ministry of Education, Science, Sports and Culture in Japan and by Japan Society for the Promotion of Science Postdoctoral Fellowships for Research Abroad.

REFERENCES

Bethe H.A., Brown G.E. 1998, ApJ, 506, 780

Cowan J.J., Pfeiffer B., Kratz K.-L., Thielemann F.-K., Sneden C., Burles S., Tytler D., Beers T.C. 1999, ApJ, 521, 194

Dunkan R.C., Shapiro S.L., Wasserman I. 1986, ApJ, 309, 141

Freiburghaus C., Rosswog S., and Thielemann F.-K. 1999, ApJ, 525, L121

Fryer, C.L., Heger, A. astro-ph/9907433

Hoffman R.D., Woosley S.E., and Qian Y.-Z. 1997, ApJ, 482, 951

Ishimaru Y. and Wanajo S. 1999, ApJ, 511, L33

Käppeler F., Beer H., Wisshak K. 1989, Rep.Prog.Phys. 52, 945

LeBlanc, J.M., Wilson, J.R. 1970, ApJ, 161, 541

McWilliam A., Preston G.W., Sneden C., Searle L. 1991, AJ, 109, 2757

Meyer B.S. 1995, ApJ, 449, L55

Nagataki, S., Hashimoto, M., Sato, K., Yamada, S. 1997, ApJ, 486, 1026

Nagataki S. 2000, ApJS, 127, 141

Otsuki K., Tagoshi H., Kajino T., and Wanajo S. 2000, ApJ, 533, 424

Qian Y.-Z., Woosley S.E. 1996, ApJ, 471, 331 (QW96)

Shapiro S.L., Teukolsky S.A. 1983 in Black Holes, White Dwarfs, and Neutron Stars (New York:John Wiely & Suns, Inc.)

Shimizu T.M, Yamada S., Sato K. 1994, ApJ, 432, L119

Sumiyoshi K., Suzuki H., Otsuki K., Terasawa M., and Yamada S. 2000, astro-ph/9912156

Symbalisty E.M.D. 1984, ApJ, 285, 729

Takahashi K., Witti J., Janaka H.-Th. 1994, A&A, 286, 857

van den Bergh S., Tammann G.A., 1991, ARA&A, 29, 363

van den Heuvel E., Lorimer D. 1996, MNRAS, 283, L37

Woods P. M., Kouveliotou C., van Paradijs J., Mark H.F., Thompson C., Duncan R.C., Hurley K., Strohmayer T., Swank J., Murakami T. 1999, ApJ, 524, L55

Woosley S.E., Wilson J.R., Mathews G.J., Hoffman R.D., and Meyer B.S. 1994, ApJ, 433, 229 (WWMHM94)

Yamada S., Sato K. 1994, ApJ, 434, 268

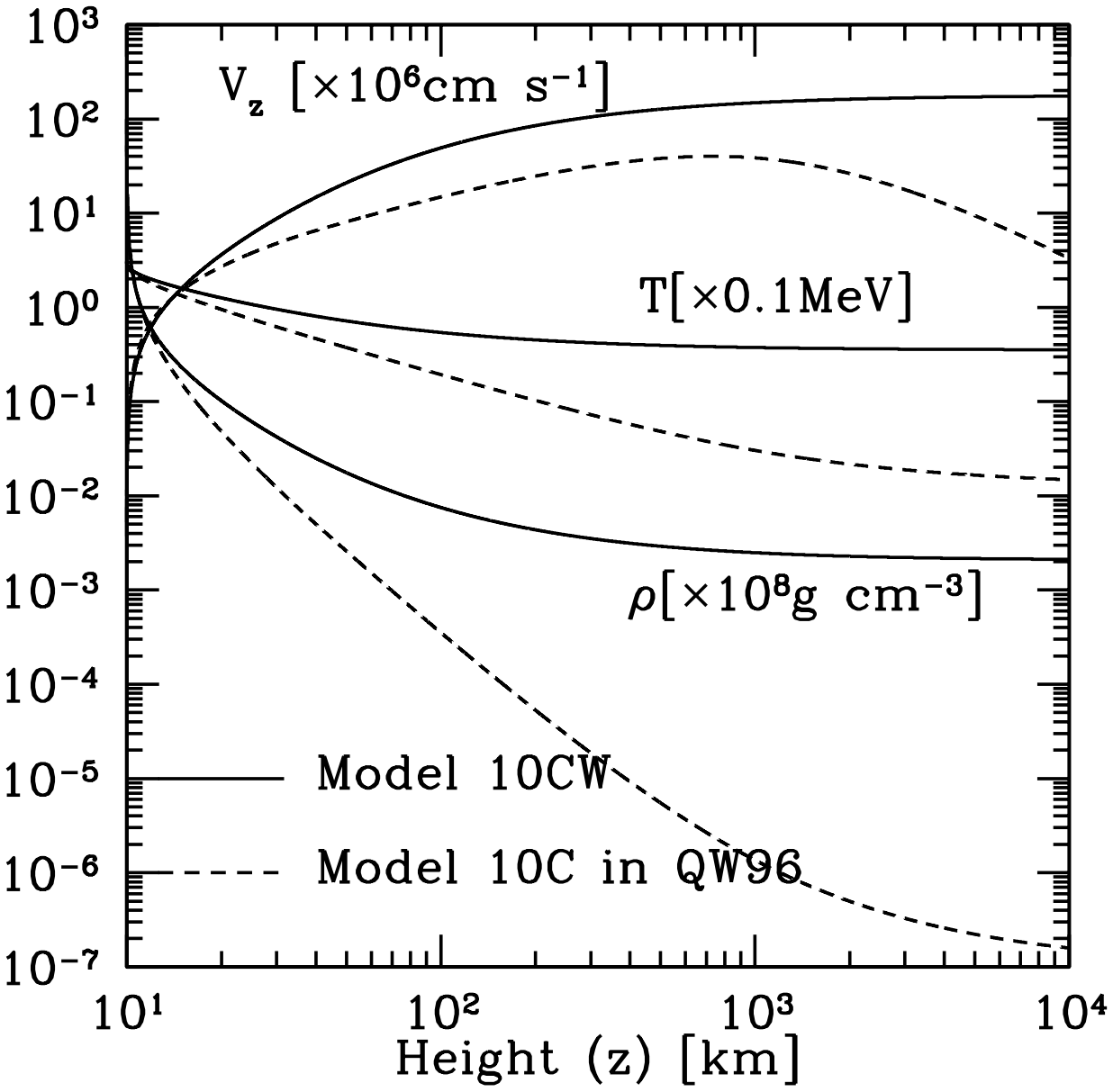

Fig. 1.— Outflow velocity, temperaure, and density as a function of height (z) from the center of the proto-neutron star. These quanta are written in unit of 10^6 cm s^{-1}, 0.1 MeV, and 10^8 g cm^{-3}, respectively. Solid lines correspond to Model 10CW, whereas dashed lines correspond to Model 10C in QW96.

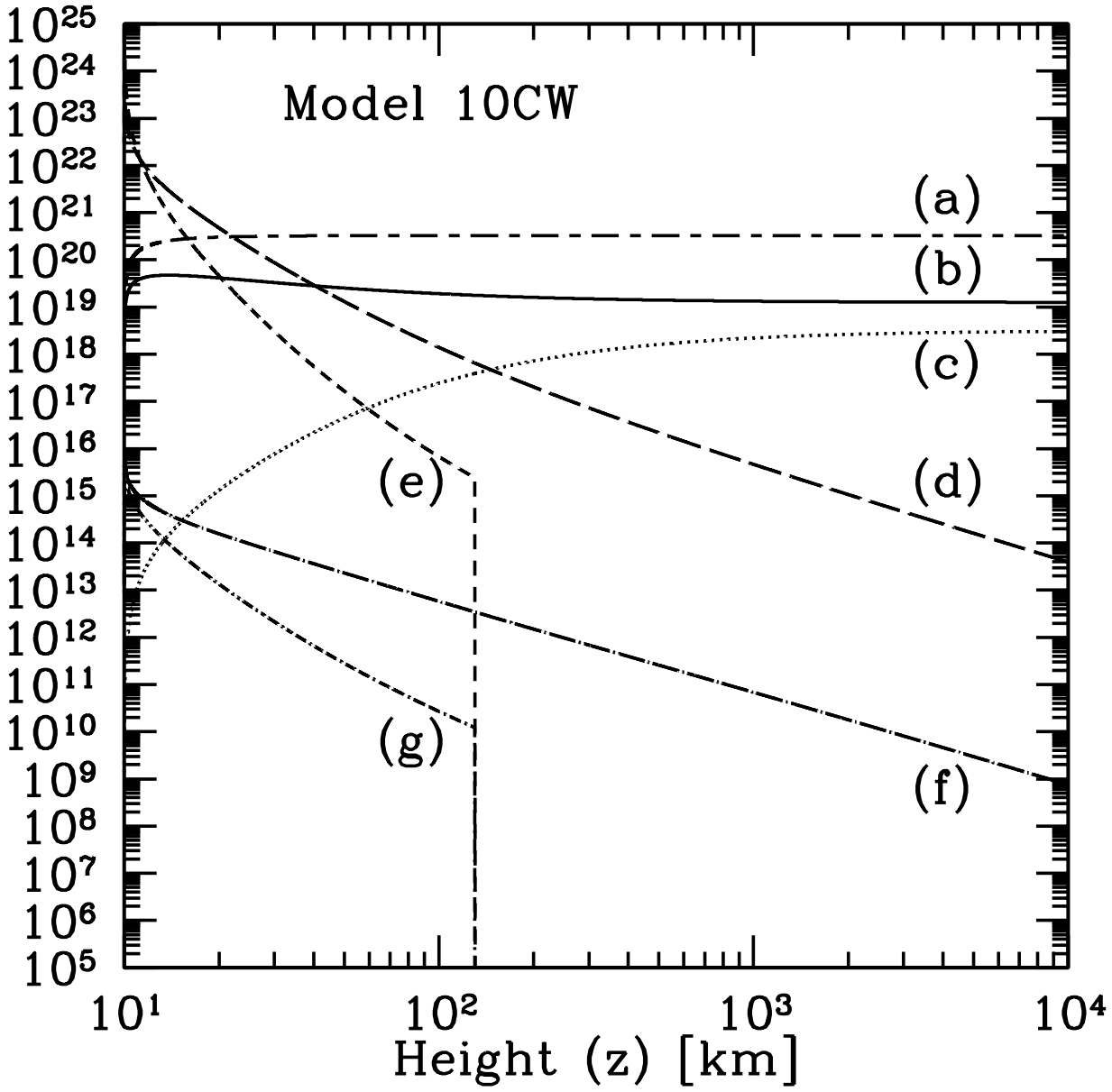

Fig. 2.— Absolute values (in cgs units) of the components of Eqs. (16) and (17) for Model 10CW. Lines (a)-(g) correspond to $4\epsilon/T$, $(P/\epsilon\rho)(\epsilon + P/\rho)$, v_z^2, $\rho GM/z^2$, $P\dot{q}/v_z\epsilon$, $(\epsilon/\rho + P/\rho^2)\frac{d\rho}{dz}$, and $\dot{q}/v_z$ as a function of z, respectively. The discontinuities of lines (e) and (g) at $z \sim 10^7$ cm reflect the freezeout of the neutrino reactions (see subsection 2.1).

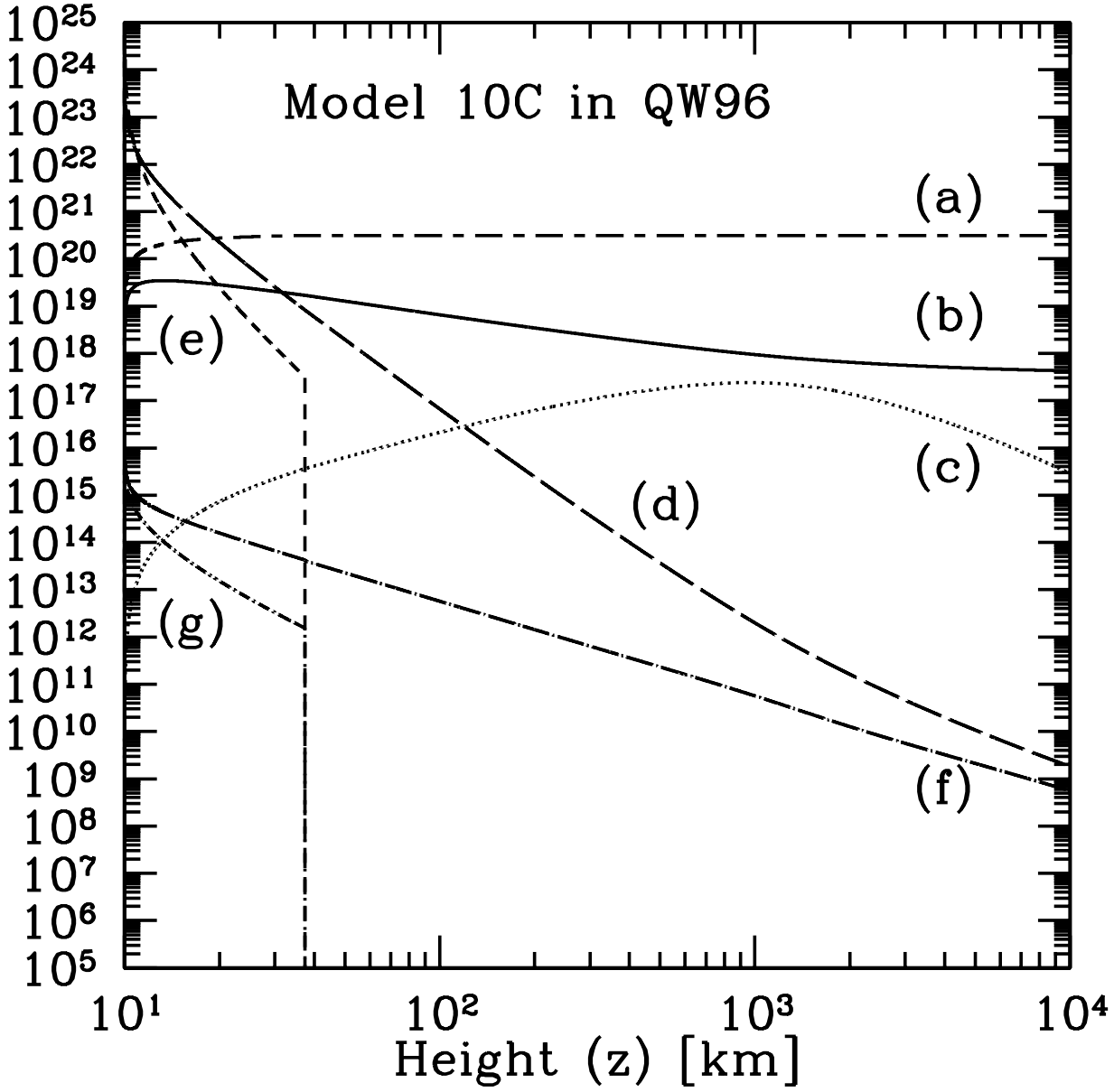

Fig. 3.— Same as Figure 2, but for Model 10C in QW96.

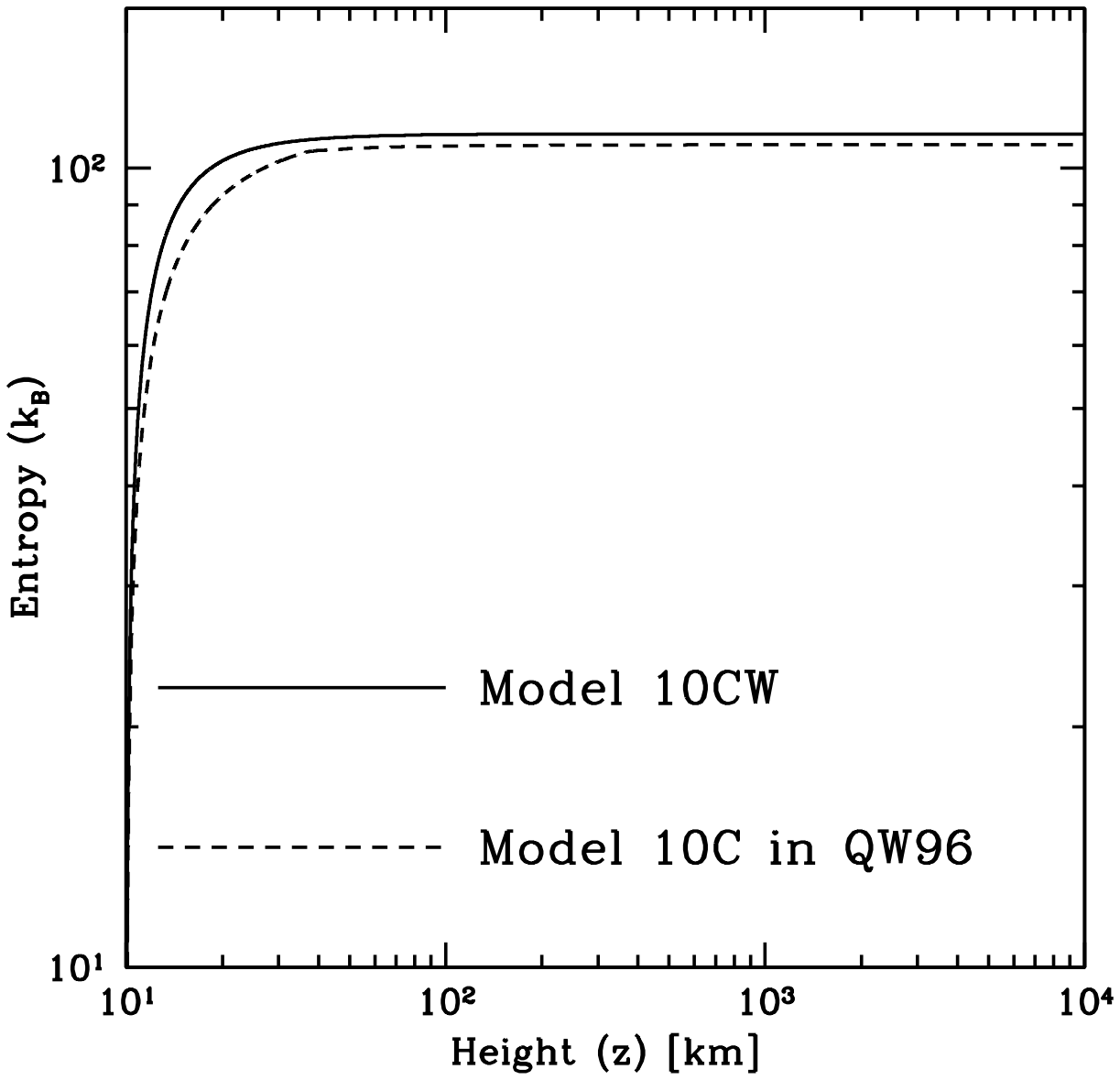

Fig. 4.— Entropy per baryon as a function of height (z) from the center of the proto-neutron star. Solid line corresponds to that of Model 10CW. Sort-dashed line corresponds to that of Model 10C in QW96.

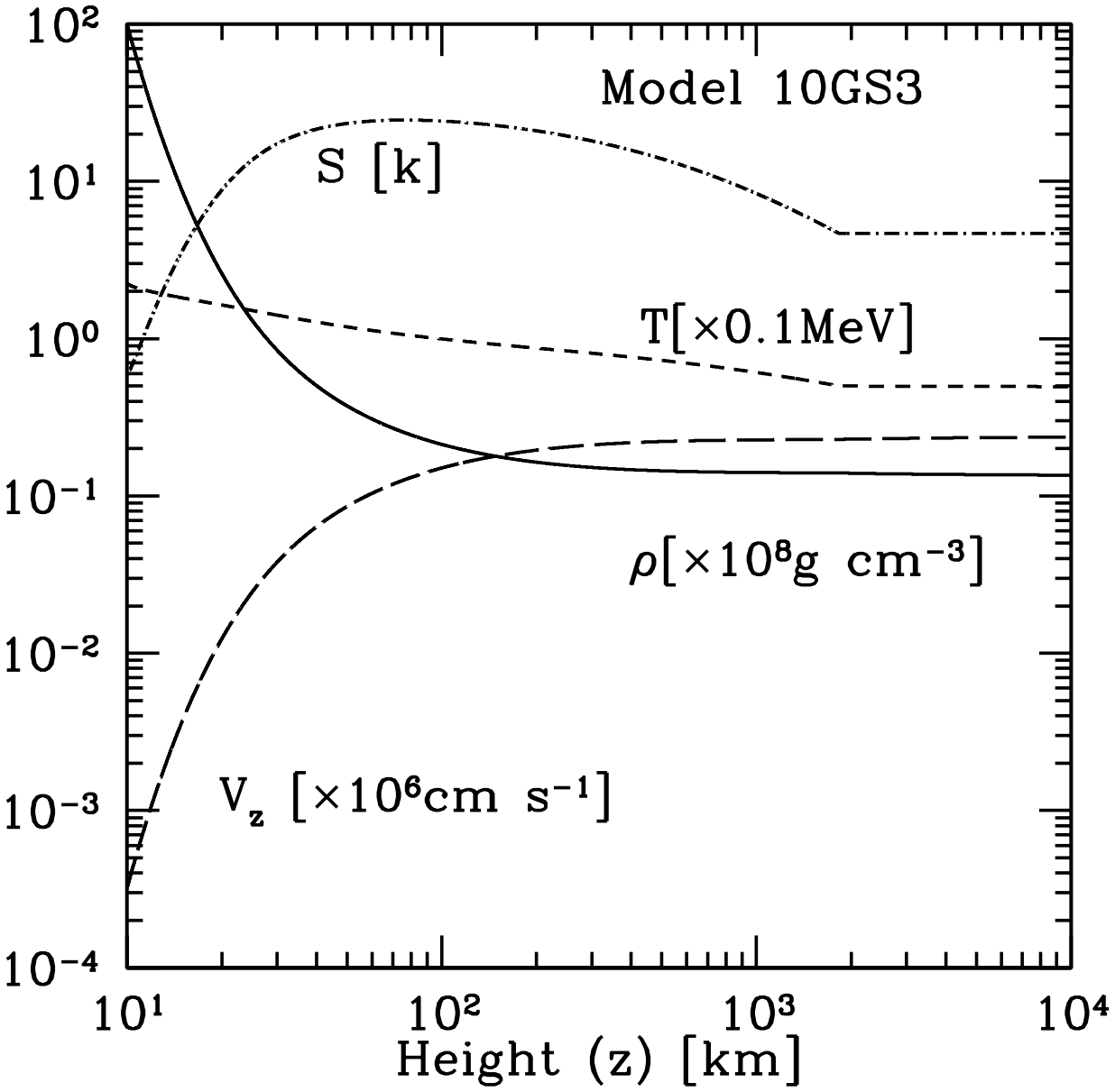

Fig. 5.— Outflow velocity, temperaure, density, and entropy per baryon as a function of height (z) from the center of the proto-neutron star in Model 10GS3. These quanta are written in unit of 10^6 cm s^{-1}, 0.1 MeV, 10^8 g cm^{-3}, and the boltzman constant, respectively.

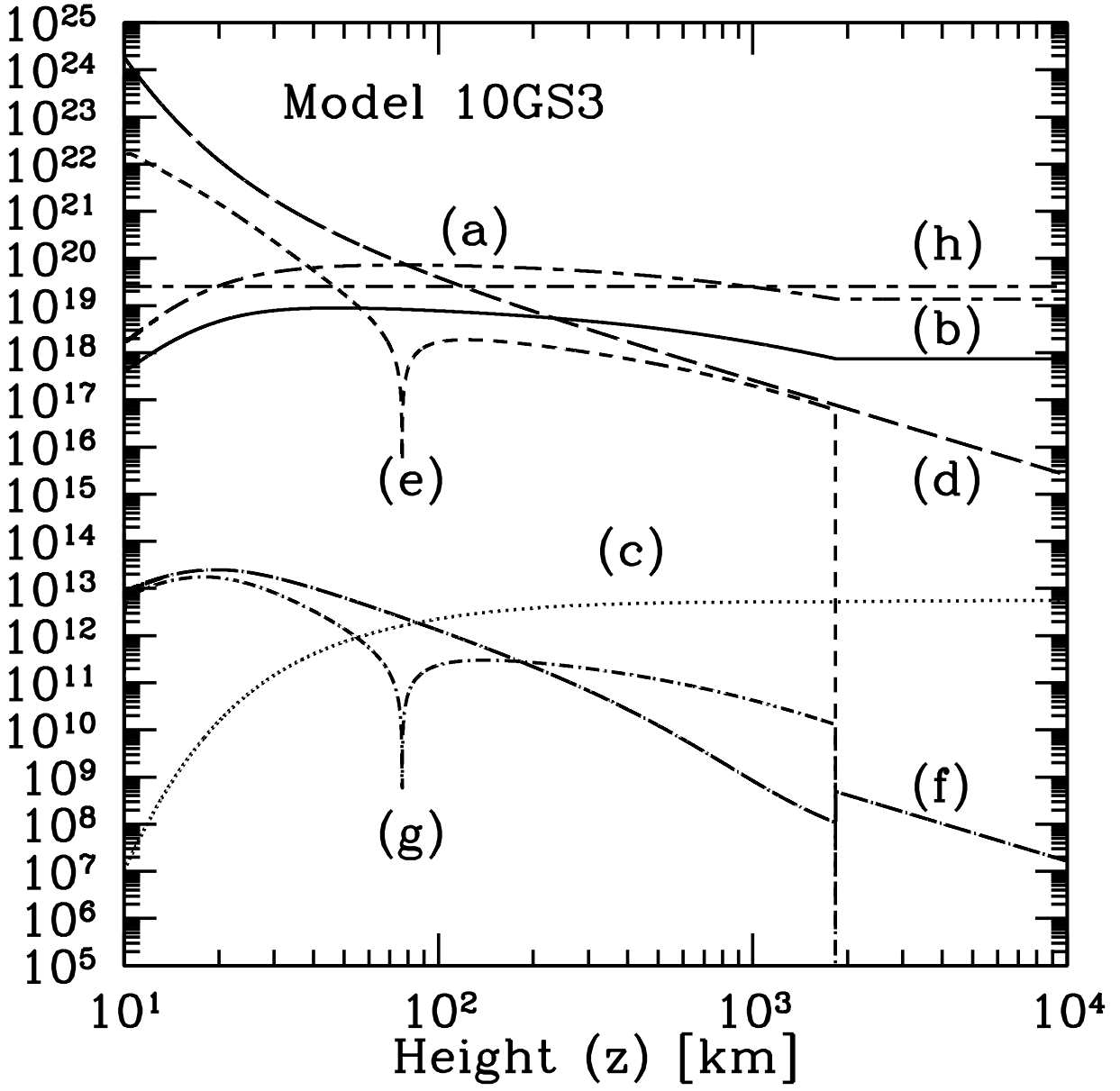

Fig. 6.— Absolute values (in cgs units) of the components of Eqs. (16) and (17) for Model 10GS3. Lines (a)-(h) correspond to $4\epsilon/T$, $(P/\epsilon\rho)(\epsilon + P/\rho)$, v_z^2, $\rho GM/z^2$, $P\dot{q}/v_z\epsilon$, $(\epsilon/\rho + P/\rho^2)\frac{d\rho}{dz}$, $\dot{q}/v_z$, and $\Omega^2 D^2/4$ as a function of height (z) from the center of the proto-neutron star, respectively. The discontinuities of lines (e) and (g) at $z \sim 8 \times 10^6$ cm and at $z \sim 2 \times 10^8$ cm reflect the change of the sign of $\dot{q}$ and freezeout of the neutrino reactions (see subsection 2.1), respectively.

Model	Mass ($M_\odot$)	Radius (km)	$L_{\bar{\nu}_e}$ (10^{51} ergs s^{-1})	$\dot{M}$ ($M_\odot$ s^{-1})	ΩD (cm s^{-1})
10AW	1.4	10	3.00	8.4(-8)	0
10BW	1.4	10	1.00	1.4(-8)	0
10CW	1.4	10	0.60	5.8(-9)	0
10DW	2.0	10	3.00	5.1(-8)	0
10EW	2.0	10	1.00	8.1(-9)	0
10FW	2.0	10	0.60	3.5(-9)	0
10GW	1.4	10	0.10	3.1(-10)	0
10GS1	1.4	10	0.10	3.1(-10)	1.0(+8)
10GS2	1.4	10	0.10	3.3(-10)	1.0(+9)
10GS3	1.4	10	0.10	5.1(-10)	1.0(+10)
10HW	1.4	10	0.05	9.8(-11)	0
10IW	1.4	10	0.01	6.6(-12)	0
10JW	2.0	10	0.10	1.8(-10)	0
10KW	2.0	10	0.05	5.7(-11)	0
10LW	2.0	10	0.01	3.9(-12)	0
30AW	1.4	30	30.0	1.3(-6)	0
30BW	1.4	30	10.0	2.2(-7)	0
30CW	1.4	30	6.00	1.1(-7)	0
30DW	1.4	30	1.00	6.0(-9)	0
30EW	1.4	30	0.50	1.9(-9)	0
30FW	1.4	30	0.10	1.4(-10)	0
30GW	1.4	30	0.05	4.4(-11)	0
30HW	1.4	30	0.01	3.0(-12)	0

Table 1: Model names and input parameters. Mass and radius of the neutron star, total luminosity of neutrinos, mass outflow rate, and ΩD are showm respectively.

Model	S (k)	$\tau_{\rm dyn}$ (s)	$\tau_{\rm dyn,ana}$ (s)	Y_e	T_b MeV
10AW	92	———	———	0.43	0.68
10BW	102	———	———	0.43	0.37
10CW	110	———	———	0.43	0.36
10DW	129	———	———	0.43	0.62
10EW	146	———	———	0.43	0.38
10FW	156	———	———	0.43	0.32
10GW	136	1.1(-1)	4.1(-2)	0.43	0.14
10GS1	137	1.1(-1)	undefined	0.43	0.15
10GS2	132	1.1(-1)	undefined	0.43	0.15
10GS3	4.7	———	undefined	0.43	0.50
10HW	150	1.7(-1)	9.4(-2)	0.43	0.11
10IW	196	1.2(-0)	7.8(-1)	0.43	9.2(-2)
10JW	196	1.2(-1)	4.8(-2)	0.43	0.12
10KW	216	2.0(-1)	1.1(-1)	0.43	0.11
10LW	274	1.2(-0)	8.9(-1)	0.43	6.1(-2)
30AW	37	———	———	0.43	1.21
30BW	42	———	———	0.43	0.92
30CW	42	———	———	0.43	0.60
30DW	50	———	———	0.43	0.31
30EW	55	———	———	0.43	0.28
30FW	64	6.5(-1)	3.6(-1)	0.43	0.11
30GW	72	1.6(-0)	9.0(-1)	0.43	0.11
30HW	90	1.1(+1)	7.9(-0)	0.43	6.8(-2)

Table 2: Model names and output parameters. Entropy per baryon, dynamical timescase ($\tau_{\rm dyn}$), analytically estimated dynamical timescale ($\tau_{\rm dyn.ana}$), electron fraction, final temperature are shown respectively. The reason why dynamical timescales are not written in some models is that temperature does not decrease to 0.2 MeV within $z = 10^9$ cm.